

Phosphotyrosine Mapping in Bcr/Abl Oncoprotein Using Phosphotyrosine-specific Immonium Ion Scanning*

Hanno Steen†, Minerva Fernandez, Saghi Ghaffari§¶, Akhilesh Pandey||, and Matthias Mann**

Bcr/Abl is a fusion oncoprotein that is of paramount importance in chronic myelogenous leukemia and acute lymphocytic leukemia. The tyrosine-phosphorylated fraction of the p185 form of Bcr/Abl was isolated by immunoprecipitation with an anti-phosphotyrosine antibody and SDS-PAGE. The tryptic digest of the gel-separated protein was prefractionated on POROS R2/OLIGO R3 microcolumns and subjected to phosphotyrosine mapping by precursor ion scanning in positive ion mode utilizing the immonium ion of phosphotyrosine, also called phosphotyrosine-specific immonium ion scanning, on a quadrupole time-of-flight tandem mass spectrometer. In total, nine different phosphorylated tyrosine residues were unambiguously localized in 12 different precursor ions. These phosphorylation sites correspond to three previously described phosphotyrosine residues and six novel tyrosine phosphorylation sites, and most of them were not predicted by the phosphorylation motif prediction programs ProSite, NetPhos, or ScanSite. This study shows the power of phosphotyrosine-specific immonium ion scanning for sensitive phosphotyrosine mapping when limited amounts of samples are available. *Molecular & Cellular Proteomics* 2:138–145, 2003.

Tyrosine phosphorylation was discovered serendipitously only 24 years ago in the course of a tumor virus study (1). Although tyrosine phosphorylation is the least abundant type of phosphorylation in eukaryotic cells compared with serine or threonine phosphorylation (probably a reason for its late discovery; relative occurrence: Ser(P), ~90%; Thr(P), ~10%; and Tyr(P), ~0.05%) (2), phosphotyrosine residues play a crucial role in receptor-mediated signal transduction affecting biological processes as diverse as cell cycle control, cell differentiation, cell movement, gene transcription, synaptic transmission, and insulin action (3). These functions require modulating inter- and intraprotein interactions via reversible protein modifica-

tions such as phosphorylation. Tyrosine phosphorylation is believed to be superior to phosphoserine and -threonine for this purpose because of the stronger binding to interaction partners facilitated by the presence of the aromatic side chain as compared with alkyl side chains (3).

Since tyrosine phosphorylation is often associated with the regulation of cell growth, it is not surprising that tyrosine kinases and phosphatases, which are often tyrosine-phosphorylated themselves, are commonly involved in oncogenesis. By the end of 2000, more than 90 distinct protein tyrosine kinase genes were identified in the human genome, and no fewer than 45 of them are involved in various types of cancer (4). Furthermore protein tyrosine phosphorylation is also associated with various other diseases ranging from septic shock to the plague (3, 5, 6). The link to cancer currently directs major research efforts toward the elucidation of phosphotyrosine-mediated signaling cascades, such as those downstream of the epidermal growth factor receptor. A major obstacle in the successful completion of these efforts is that analysis of tyrosine-phosphorylated proteins can be quite challenging.

Regulatory proteins are typically of low natural abundance within a cell. Additionally *in vivo* signaling through reversible phosphorylation of proteins is often achieved at low phosphorylation stoichiometries. From an analytical point of view, these two factors dictate that the analytical strategy used for phosphotyrosine mapping must be as sensitive as possible. Given practical limits with regard to starting amounts of cells, it should work at a low to subpicomole scale.

Recently we devised a strategy for the selective detection of tyrosine-phosphorylated peptide without the interference of the much more abundant serine- and/or threonine-phosphorylated peptides (7, 8). This method is based on precursor ion scanning in positive ion mode and uses the immonium ion of phosphotyrosine at m/z 216.043 as characteristic reporter ion and was thus named PSI¹ scanning for phosphotyrosine-specific immonium ion scanning. Due to the presence of numerous other fragment ions with the same nominal but

From the Center for Experimental Bioinformatics, Department of Biochemistry and Molecular Biology, University of Southern Denmark, 5230 Odense M, Denmark and the §Whitehead Institute for Biomedical Research and Massachusetts Institute of Technology, Cambridge, Massachusetts 02142

Received, January 9, 2003, and in revised form, February 25, 2003
Published, MCP Papers in Press, February 25, 2003, DOI 10.1074/mcp.M300001-MCP200

¹ The abbreviations used are: PSI, phosphotyrosine-specific immonium ion; CML, chronic myelogenous leukemia; ALL, acute lymphocytic leukemia; MS, mass spectrometry; MS/MS, tandem MS; pY, phosphotyrosine; Mox, oxidized methionine.

slightly different exact masses, high resolution, high accuracy mass spectrometers such as quadrupole time-of-flight hybrid instruments are required for this approach. The applicability of PSI scanning for the sensitive analysis of low abundance tyrosine-phosphorylated signaling proteins was recently shown by the mapping of phosphotyrosine residues in the epidermal growth factor and fibroblast growth factor receptor signaling pathways (9, 10), which identified in an unbiased approach numerous novel tyrosine phosphorylation sites in addition to the well characterized ones.

In this study we applied PSI scanning to the phosphotyrosine mapping of Bcr/Abl. Bcr/Abl is a fusion oncoprotein that is of paramount importance in chronic myelogenous leukemia (CML) and acute lymphocytic leukemia (ALL). The fusion is the consequence of a reciprocal translocation between the long arms of chromosomes 9 and 22 resulting in a truncated chromosome 22, called the Philadelphia chromosome (11). It can be found in more than 90% of CML and in up to 20% of adult ALL patients depending on the isoform of Bcr/Abl (12). The oncogene comprises the major part of the *bcr* gene at its 5'-end and the major part of the *c-abl* gene at its 3'-end. The *c-abl* gene encodes for a tightly controlled tyrosine kinase that becomes constitutively active in the *bcr/abl* gene product (a severalfold increase in activity (13)). Although the actual mechanism of the induction of CML and ALL by Bcr/Abl is still unclear, there is evidence that the disease state is not only the result of simple growth factor activation but that apoptosis suppression is involved as well (13, 14). The connection between Bcr/Abl and CML and/or ALL has been known for several years. Yet new interest was aroused recently when a highly potent and selective Abl kinase inhibitor was synthesized by Zimmermann *et al.* (15). The molecule proved to be a promising lead compound resulting in the synthesis of a derivative named STI-571 (Gleevec) (12, 16). STI-571 is approved as an anticancer drug because of very positive results in clinical trials. Due to this, major research efforts are underway to further elucidate the modifications, structure, and function of this oncogenic fusion protein (see e.g. Ref. 16). Several isoforms of the Bcr/Abl protein have been described as showing different activities and different distributions in the various forms of leukemia (12). p185 (also called p180), the isoform of Bcr/Abl with the highest kinase activity (13), was chosen for tyrosine phosphorylation mapping by PSI scanning. The expression of this particular isoform is considered as the cause of Philadelphia+ ALL. Here we report numerous novel tyrosine phosphorylation sites in addition to the ones described in the literature.

MATERIALS AND METHODS

Immunoprecipitation—A total of 3×10^7 human embryonic kidney 293T cells were grown in Dulbecco's modified Eagle's medium containing 10% fetal bovine serum. Cells were transfected with p185 Bcr/Abl cDNA using the calcium phosphate method. After transfection the cells were grown to 80% confluence and then cultured for an additional 15 h without serum. Cells were lysed in ice-cold lysis buffer

containing 50 mM Tris-HCl (pH 7.4), 150 mM NaCl, 1 mM EDTA, 1% Nonidet P-40, 0.25% sodium deoxycholate, and 1 mM sodium orthovanadate in the presence of protease inhibitors. The lysates were pooled and cleared by centrifugation (14,000 rpm for 15 min). Cleared lysates were incubated overnight with gentle rocking at 4 °C using 50 μ g of 4G10 anti-phosphotyrosine antibody (Upstate Biotechnology) coupled to agarose beads. The precipitated immune complex was washed three times with 1 ml of lysis buffer followed by pelleting the agarose beads at 4000 rpm after each wash (17). Subsequently the beads were boiled in SDS loading buffer for 5 min, and the proteins were resolved by SDS-PAGE (10% gel) prior to silver staining as described previously (18).

Sample Preparation—The gel band of interest was excised and subjected to in-gel reduction, alkylation, and tryptic digestion according to described procedures (18), and the peptide mixture was loaded onto a double microcolumn of POROS R2 and OLIGO R3 material (Applied Biosystems, Framingham, MA) packed into GE-Loader tips (Eppendorf, Hamburg, Germany) as described previously by Neubauer and Mann (19). The fractionated peptide mixture was desalted by washing each column with 10 μ l of 5% formic acid followed by step elution with 20 and 40% methanol in 5% formic acid directly into nanoelectrospray needles (Proxeon Biosystems A/S, Odense, Denmark) and subjected to mass spectrometric analysis.

Mass Spectrometry—All experiments were performed on a QSTAR Pulsar quadrupole time-of-flight mass spectrometer (AB/MDS Sciex, Toronto, Canada) equipped with a nanoelectrospray ion source (Proxeon). Precursor ion scans were acquired with a dwell time of 50 ms at a step size of 0.5 Da and with the Q_2 pulsing function turned on. Nitrogen was used as the collision gas at a recorded pressure of 5.3×10^{-5} Torr. The collision energy was ramped over the m/z range proportional to one-tenth of the m/z value of the precursor ion, *i.e.* the collision energy was ramped from 35 to 100 V for the normally used scan range of m/z 350–1000.

RESULTS AND DISCUSSION

The Bcr/Abl p185 DNA was transfected into 293T cells for transient expression prior to immunoprecipitation of the tyrosine-phosphorylated proteins with immobilized 4G10 anti-phosphotyrosine antibody. The obtained protein mixture was separated by SDS-PAGE and visualized by silver staining. The gel image is shown in Fig. 1. As expected one main protein band at \sim 185 kDa was apparent (marked with an *arrow*) that was tentatively assigned as tyrosine-phosphorylated p185 Bcr/Abl protein.

This gel band was excised and subjected to in-gel digestion prior to mass spectrometric analysis for protein identification and phosphotyrosine mapping with the PSI scanning approach. The mass spectrum of the first elution (20% methanol, 5% formic acid) of the POROS R2 fraction did not show many peptide ion signals, and the precursor-of- (m/z 216.045 ± 0.025) experiment also did not reveal any ion signals (data not shown). The elution with 40% methanol, 5% formic acid produced a mass spectrum of a complex peptide mixture as shown in Fig. 2A. Subsequently precursor ion experiments were performed. A nonspecific precursor ion scan (m/z 216.0 ± 0.5) for comparison purposes and a specific precursor-of- (m/z 216.045 ± 0.025) experiment are shown in Fig. 2, B and C. The former precursor ion experiment also detects those precursors that give rise to interfering fragment ions with the

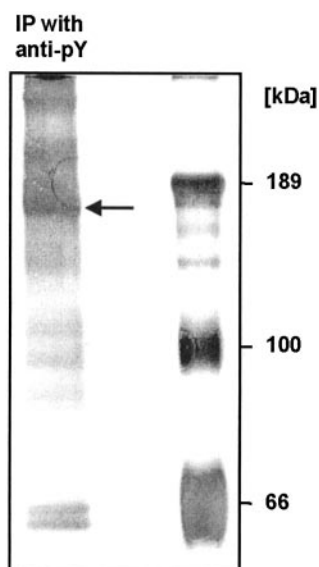


FIG. 1. Purification of the p185 isoform of Bcr/Abl by SDS-PAGE. 293T cells were transfected to express the p185 isoform of Bcr/Abl. All phosphotyrosine-containing proteins were immunoprecipitated with an immobilized anti-phosphotyrosine antibody and separated by SDS-PAGE. Silver staining showed that a protein with a mass expected for the p185 isoform was the major tyrosine-phosphorylated species. This band (indicated with an *arrow*) was excised and in-gel digested with trypsin for further mass spectrometric analysis.

same nominal but slightly different exact masses at around m/z 216. Comparing these two spectra, it was obvious that several of the major ion signals in the nonspecific precursor ion experiment did not correspond to phosphotyrosine-containing peptides. The highly specific PSI scan revealed 12 major ion signals apart from numerous smaller signals. Inspecting the mass spectrum of the peptide mixture at the appropriate m/z ranges revealed mainly ion signals corresponding to triply and quadruply charged peptides. The charge state of some precursors could not always be derived from the survey mass spectrum because of isobaric interferences. For instance, the specific precursor ion spectrum showed a clear signal in the range of m/z 541. The mass spectrum showed a quintuply charged species at m/z 540.8, a doubly charged species at m/z 541.3, and a triply charged species at m/z 541.6 in the corresponding m/z range such that it was not possible to state which of these species contained the phosphotyrosine residue. All of these ions could have given rise to the phosphotyrosine immonium ion at m/z 216.045. Only the charge states of the main fragment ions that unambiguously localized the phosphotyrosine residue allowed the conclusion that the quintuply charged species marked with an *arrow* in Fig. 2D was indeed the precursor of interest. Interpretation of the product ion spectrum revealed the phosphorylation of Tyr-177, a well described Grb2-binding site (20–22) (data not shown). This unambiguous localization of the phosphorylation site in this highly charged precursor

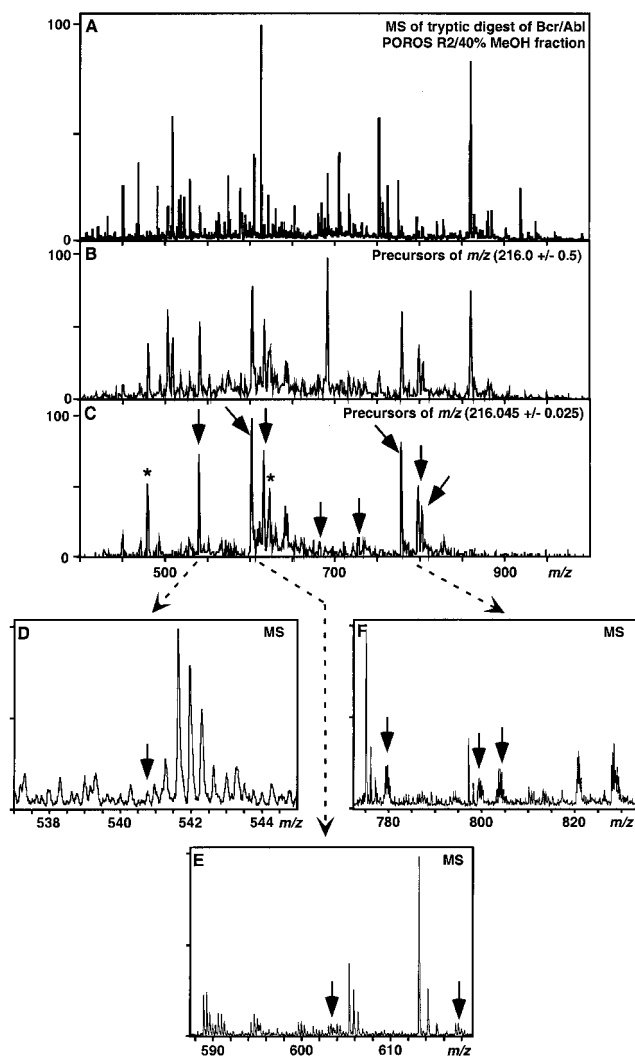


FIG. 2. Mass spectrometric analysis of the POROS R2/40% methanol fraction. A, mass spectrum of the tryptic in-gel digest of Bcr/Abl eluted from the POROS R2 microcolumn with 40% methanol, 5% formic acid. B, the nonspecific precursor ion spectrum displayed numerous prominent ion signals. C, the specific precursor-of- $(m/z$ 216.045 \pm 0.02) experiment shows that only some of the ion signals were attributable to phosphotyrosine-containing peptides. The ion signals marked with an *arrow* correspond to precursors that were subjected to MS/MS analysis providing product ion spectra that allowed the localization of tyrosine phosphorylation sites. The ion signals marked with an *asterisk* indicate precursors that did not provide sufficient data upon collision-induced dissociation for phosphotyrosine localization. D–F, expansions of several m/z ranges where precursors gave rise to ion signals in the specific precursor ion experiment. Precursors subjected to MS/MS analysis are marked with *arrows*.

was only possible because of the high resolution and high accuracy provided by the quadrupole time-of-flight mass spectrometer, which allowed the assignment of the differently charged peptide fragment ions series. In total 10 precursors detected by PSI scanning in the POROS R2/40% methanol fraction were subjected to MS/MS experiments. Eight of these

TABLE I
Result of the phosphotyrosine mapping in Bcr/Abl

Listed are the phosphotyrosine residues that were localized as well as the corresponding phosphopeptide sequence, observed m/z value, z value, and expected molecular weight.

m/z	z	M_r (theoretical)	Peptide sequence	Residue nos. (Tyr(P))
40% methanol, 5% formic acid elution of POROS R2				
541.2	5	2700.19	GHGQPGADA EKPFp YVNVEFHHER	164–186 (177)
676.1	4	2700.19	GHGQPGADA EKPFp YVNVEFHHER	164–186 (177)
728.3	3	2182.02	NGQGWWPSN pY ITPVNSLEK	506–524 (515)
603.0	4	2408.06	NKPTV pY GVSPNYDKWEMoxER	621–639 (626)
803.7	3	2408.06	NKPTV pY GVSPNYDKWEMoxER	621–639 (626)
779.3	4	3113.40	NKPTV pY GVSPNYDKWEMoxERTDITMoxK	621–645 (626)
799.3	4	3193.35	NKPTV pY GVSPN pY DKWEMoxERTDITMoxK	621–645 (626 + 632)
617.3	3	1848.84	LGGGQ pY GEVYEGVWKK	648–663 (653)
			LGGGQYGEV pY EGVWKK	648–663 (657)
20% methanol, 5% formic acid elution of OLIGO R3				
480.7	2	959.47	pY SLTVAVK	664–671 (664)
40% methanol, 5% formic acid elution of OLIGO R3				
602.9	3	1805.82	INTASDGK LpY VSSSESR	576–591 (585)
643.3	3	1928.81	LGGGQ pY GEV pY EGVWKK	648–663 (653 + 657)
511.5	3	1515.64	LMoxTGDT pY TAHAGAK	787–800 (793)

10 product ion spectra allowed precise localization of the tyrosine phosphorylation sites (see Fig. 2, marked with *arrows*). The other two product ion spectra were of inadequate quality and did not provide data that allowed the assignment of either a peptide sequence or a phosphorylation site (marked with *asterisks*). This observation demonstrates that the sensitivity of precursor ion experiments is superior to normal MS or MS/MS experiments (23).

The base peak in the specific PSI spectrum had an m/z value of ~ 603 . A minor quadruply charged precursor was identified in the mass spectrum of the digest in the corresponding m/z region (see Fig. 2E, *left arrow*). Product ion experiments revealed the presence of the phosphorylated tryptic peptide T-(621–639), NKPTV**pY**GVSPNYDKWEMoxER, where pY is phosphotyrosine and Mox is oxidized methionine (data not shown). Due to the presence of two tyrosine residues within this peptide, sequence information was indispensable in unequivocally allocating the phosphorylation to Tyr-626. This phosphorylation of Tyr-626 was confirmed by product ion spectra of the precursors at m/z 803.7 and 779.3, the former being the corresponding triply charged precursor and the latter being a longer quadruply charged peptide comprising the same phosphotyrosine residue in addition to a miscleaved trypsin cleavage side (see Table I). Interestingly the product ion spectra of all these monophosphorylated precursors at m/z 603.0, 803.7, and 779.3 clearly show phosphorylation of Tyr-626 but no evidence for the phosphorylation of the other tyrosine residue (Tyr-632). Nevertheless the fact that the second tyrosine residue (Tyr-632) could also be phosphorylated was shown by the product ion spectrum of the quadruply charged precursor at m/z 799.3 (T-(621–645),

NKPTV**pY**GVSPN**pY**DKWEMoxERTDITMoxK; see Fig. 3); both phosphorylated tyrosine residues were unambiguously assigned based on a doubly charged y -type fragment ion series. These findings about Tyr-626 and Tyr-632 might indicate that the phosphorylation of these two tyrosine residues does not occur in a random but ordered fashion; however, additional quantitative experiments are required to investigate this further.

The product ion spectrum of the triply charged precursor at m/z 617.3 revealed that the precursor corresponds to the singly phosphorylated tryptic peptide T-(648–663), LGGGQYGEVYEGVWKK, containing two tyrosine residues. A thorough interpretation of the data to allocate the phosphorylation site revealed two y -type fragment ion series that coincide with cleavages flanking the two tyrosine residues. However, for cleavages between the two tyrosine residues, two fragment ion series 80 Da apart are present (see Fig. 4). These data indicate the partial phosphorylation of both tyrosine residues (Tyr-653 and Tyr-657), *i.e.* the precursor at m/z 617.3 presented a mixture of two isomeric peptides that only differed in the position of the phosphotyrosine residue. The comparable intensity of the fragment ion pairs points to similar phosphorylation of both tyrosine residues. PSI scanning followed by peptide sequencing thus allows the unambiguous differentiation between different types of phosphopeptides with two tyrosine residues: (i) only one particular tyrosine residue is phosphorylated, (ii) both tyrosine residues are phosphorylated, and (iii) a mixed population of two different singly phosphorylated peptides with the same amino acid sequence is present.

To check whether the minor ion signals observed in the

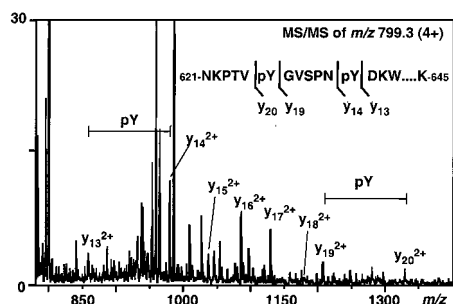


FIG. 3. Product ion spectra of a tyrosine-phosphorylated peptide derived from Bcr/Abl. Shown is the product ion spectrum of the quadruply charged doubly tyrosine-phosphorylated tryptic peptide T-(621–639) at m/z 799.3: NKPTVpYGVSPNpYDKWEMoxERTDIT-MoxK.

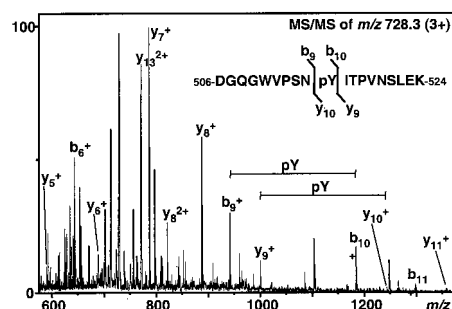


FIG. 5. Product ion spectrum of a tyrosine-phosphorylated peptide derived from Bcr/Abl. Shown is the product ion spectrum of the triply charged, singly phosphorylated tryptic peptide at m/z 728.3, which only gave rise to a minor ion signal in the specific precursor ion experiment (see Fig. 2C): T-(506–524), NGQGWVPSNpYITPVNSLEK.

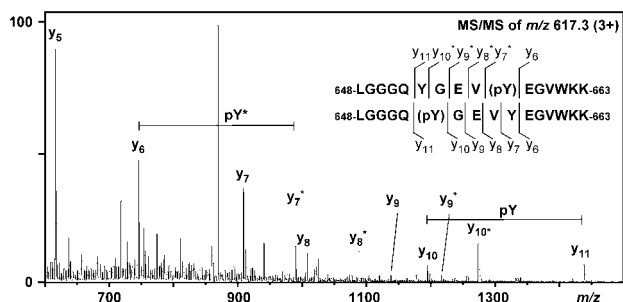


FIG. 4. Product ion spectrum of two isomeric tyrosine-phosphorylated peptides derived from Bcr/Abl. Shown is the product ion spectrum of the precursors at m/z 617.3 (3+). Two fragment ion series were visible and attributable to the two isomeric singly phosphorylated peptides LGGGQpYGEVYEGVWKK and LGGGQYGEVpYEGVWKK (T-(648–663)).

selective precursor ion experiment indeed represented tyrosine-phosphorylated peptides, two other peptides, which gave rise to these minor ion signals in the precursor-of-(m/z 216.045 \pm 0.025) spectrum, were sequenced (marked with arrows in Fig. 2C). These two ion signals were also attributable to phosphotyrosine-containing peptides. The precursor at m/z 676.1 corresponded to the quadruply charged counterpart of the monophosphorylated tryptic peptide T-(164–186) (see above). The fragmentation of the other low intensity ion signal at m/z 728.3 proved that Tyr-515 of the tryptic peptide T-(506–524), DGQGWVPSNpYITPVNSLEK, was phosphorylated (see Fig. 5). Furthermore it showed that the amino acid residue at position 506 corresponded to an aspartate and not to an asparagine residue. Additional experiments are required to clarify whether this deamidation is a random and artificial event or whether it is of biological importance as it has been shown that deamidation at particular asparagine residues can be of paramount importance for the function of proteins (24).

Due to limited sample volume and the resulting time constraints in the nano-electrospray experiment, sequencing additional observed precursors in the selective precursor ion spectrum from the POROS R2/40% methanol fraction was not possible. Therefore some of the potentially tyrosine-phosphorylated precursors detected in that precursor ion experi-

ment remained unidentified. However, additional tyrosine phosphorylation sites were localized when the peptides that were bound to the OLIGO R3 material (the more hydrophilic fraction) were analyzed. The results of the product ion experiments described below are summarized in the lower part of Table I.

The mass spectrum of the OLIGO R3/20% methanol fraction is shown in Fig. 6A. The precursor-of-(m/z 216.045 \pm 0.025) spectrum of this fraction showed one intense ion signal at m/z 480 (see Fig. 6B). The inset in Fig. 6A shows the position of the respective ion species, giving rise to the intense ion signal in the precursor-of-(m/z 216.045 \pm 0.025) experiment, indicating the low signal to noise ratio of the ion signal of this phosphopeptide.

Fragmentation of the precursor ion at m/z 480.7 (doubly charged) showed the presence of a singly phosphorylated peptide covering the sequence stretch 664–671 with a phosphorylated tyrosine residue at its N terminus (see Fig. 6C). It is interesting to note that the activity of trypsin is severely inhibited by a phosphorylated amino acid in the +2-position with respect to an arginine or lysine residue (25, 26) but that in this case the presence of the phosphorylated tyrosine residue just C-terminal to the Arg or Lys residue (+1-position) did not seem to severely affect the cleavage efficiency of trypsin.

The survey mass spectrum and the low and high resolution precursor ion spectra of the OLIGO R3/40% methanol fraction are shown in Fig. 7, A–C. Numerous ion signals can be found in the survey mass spectrum, whereas the high resolution precursor-of-(m/z 216.045 \pm 0.025) experiment of this fraction displayed the same major ion signal at m/z 470 as the OLIGO R3/20% methanol fraction. In addition, three minor ion signals that were previously obscured by nonspecific ion signals in the low resolution precursor ion experiment are observable (see Fig. 7, B and C, marked with arrows). These three precursors were subjected to additional product ion experiments (m/z 511.5, 602.9, and 643.3). The precursors at m/z 511.5 and m/z 602.9 were identified as corresponding to the tryptic peptides T-(787–800), LMoxTGDTpYTAHAGAK (Fig. 7D), and T-(576–591), INTASDGKlpYVSSSR (Fig. 7E),

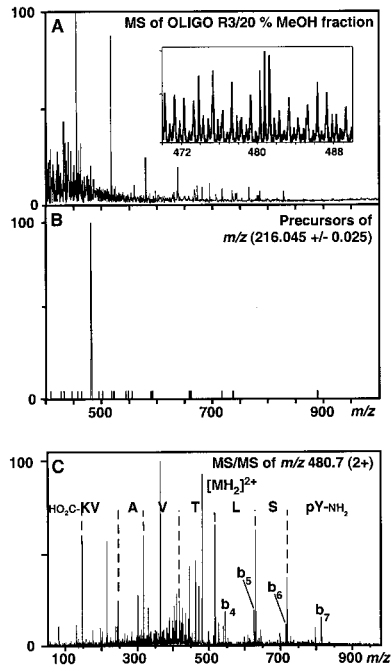


FIG. 6. Mass spectrometric analysis of the OLIGO R3/20% methanol fraction of the Bcr/Abl digest. *A*, mass spectrum of the tryptic in-gel digest of Bcr/Abl eluted from the OLIGO R3 microcolumn with 20% methanol, 5% formic acid. The inset in *A* shows the signal intensity of the precursor giving rise to the prominent ion signal at m/z 481 in *B*, the specific precursor-of- $(m/z$ 216.045 ± 0.025) experiment. *C*, product ion spectrum of the doubly charged tryptic peptide T-(664–671), pYSLTVAVK.

respectively, identifying two additional tyrosine phosphorylation sites at Tyr-793 and Tyr-585. Tyr-793 is a well characterized autophosphorylation site (27). A triply charged precursor at m/z 643.3 was also found and could be attributed to the doubly phosphorylated peptide T-(648–663), LGGGQpY-GEVpYEGVWKK (data not shown). The singly phosphorylated counterparts of the peptide T-(648–663) had already been analyzed in the POROS R2/40% methanol fraction (see above).

Several tyrosine phosphorylation sites have been described previously for Bcr, Abl, and the fusion protein Bcr/Abl. Tyr-245 and Tyr-412 have been reported as Abl phosphorylation sites (27) (these correspond to Tyr-626 and Tyr-793 in the Bcr/Abl (p185) sequence), and Tyr-177, Tyr-283, Tyr-328, and Tyr-360 have been identified as being phosphorylated in Bcr (22). However, only Tyr-177, Tyr-283, and Tyr-360 were identified as phosphorylated residues specific to the fusion protein Bcr/Abl (20, 21), and the latter two have only been observed in samples subjected to *in vitro* phosphorylation. The results of this study described in the previous section confirmed the one known *in vivo* phosphorylation site of Bcr/Abl and the two phosphotyrosine residues described for Abl. In addition six new phosphorylation sites were identified.

Mass spectrometry (without internal standards) can only confirm the presence of a particular phosphorylation site but

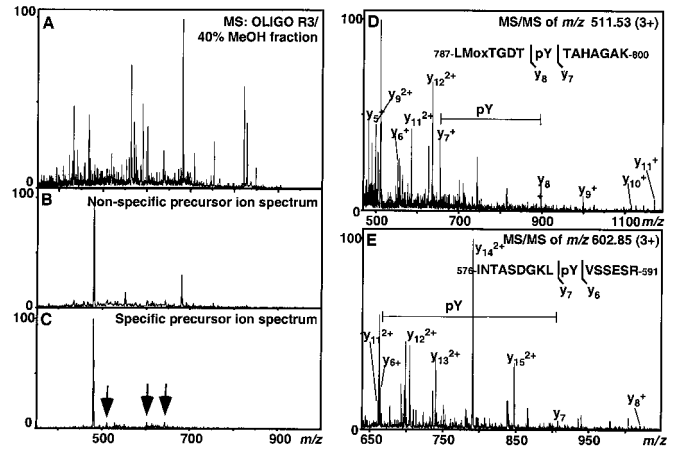


FIG. 7. Mass spectrometric analysis of the OLIGO R3/40% methanol fraction of the Bcr/Abl digest. *A*, mass spectrum of the tryptic in-gel digest of Bcr/Abl eluted from the OLIGO R3 microcolumn with 20% methanol. *B*, the nonspecific precursor ion spectrum showed two additional ion signals as well as the major ion signal at m/z 481 (see Fig. 6). *C*, the specific precursor-of- $(m/z$ 216.045 ± 0.025) experiment shows that these two ion signals are not correlated with tyrosine-phosphorylated peptides. Some minor ion signals were observable (marked with arrows). *D*, product ion spectrum of the triply charged tryptic peptide at m/z 511.5: T-(787–800), LMoxTGDTpY-TAHAGAK. *E*, product ion spectrum of the triply charged tryptic peptide at m/z 602.9: T-(576–591), INTASDGKLPYVSSSESR. The precursors of the spectra shown in *D* and *E* only gave rise to ion signals of low intensity in *C*.

does not necessarily indicate the absence of a site, and this study suffers from the same limitations as any other modification study that uses only one protease: no complete sequence coverage is obtained as peptides are lost during the sample work-up, or they are not observed due to low ionization efficiency, ionization suppression, or size limitations (28). Therefore we cannot state from our data set that the other phosphorylation sites described for Bcr, Abl, and/or Bcr/Abl are not present under the biological conditions of this experiment. The size limitation excludes for instance a quarter of all tyrosine-containing peptides derived from a tryptic digest of p185 as they are well below 700 Da or above 3200 Da, which is outside the mass range normally observed in standard nano-electrospray experiments with limited amounts of protein digests. The size limitation is also the most probable reason why no information was obtained for the peptides containing residues Tyr-283 and Tyr-328; both potential phosphorylation sites are located in tryptic peptides with masses above 3.5 kDa (assuming no miscleavages), *i.e.* above the normally observed mass range. Additional experiments using *e.g.* different endoproteases are required to address the questions (i) whether the other tyrosine residues are indeed not phosphorylated under the given conditions, (ii) whether the tyrosine residues were phosphorylated but to such a low extent that the dynamic range and detection limit of the applied technique was insufficient, or (iii) whether the other tyrosine phosphorylation sites were simply missed in this study.

TABLE II
Prediction of phosphotyrosine residues in Bcr/Abl

Listed are the results of the different tyrosine phosphorylation prediction programs. The following prediction programs were used: ProSite (www.isrec.isb-sib.ch/software/PFSCAN_form.html), NetPhos 2.0 (www.cbs.dtu.dk/services/NetPhos/), and ScanSite (scansite.mit.edu/). The observed phosphotyrosine residues are marked with a + if predicted and a – if not predicted.

Tyr(P) residue	NetPhos	ProSite	ScanSite (stringency)		
			Low	Medium	High
			177	+	–
515	–	–	+	–	–
585	+	–	–	–	–
626	–	–	+	–	–
632	–	–	–	–	–
653	–	–	+	–	–
657	+	–	+	+	–
664	–	–	–	–	–
793	+	–	–	–	–
No. of predicted Tyr(P) sites	10	0	10	4	1

During the review process of this manuscript a phosphorylation study on CML cells in response to inhibition by STI-571/Gleevec was published by Salomon *et al.* (29). The results from this study corroborate our data as four of the six novel tyrosine phosphorylation sites identified in our study on p185 (Tyr-585, Tyr-653, Tyr-657, and Tyr-664 in p185) were also found for p210-expressing cells using an immobilized metal affinity chromatography-liquid chromatography-MS approach for phosphorylation analysis; p210 is the Bcr/Abl isoform leading to CML. In addition, a tyrosine residue corresponding to Tyr-869 in p185 was observed to be phosphorylated. However, no phosphopeptides containing phosphotyrosine residues Tyr(P)-515 and Tyr(P)-632 were observed in contrast to our study. The fact that most of the tyrosine phosphorylation sites were found in both our tyrosine phosphorylation study of overexpressed p185 and in the study of Salomon *et al.* (29) using a system that expresses p210 at an endogenous level underscores the potential importance of these tyrosine phosphorylation sites *in vivo*.

To compare the experimentally determined phosphotyrosine residues with predicted phosphotyrosine motifs, the Bcr/Abl (p185) sequence was interrogated with ProSite (www.isrec.isb-sib.ch/software/PFSCAN_form.html), NetPhos (www.cbs.dtu.dk/services/NetPhos/) (30), and ScanSite (scansite.mit.edu/) (31) (see Table II). ProSite has a tendency to underpredict tyrosine phosphorylation sites since it only utilizes the motifs RXX₂DEX₃Y or RXX₃DEX₂Y (where Y indicates the phosphorylation site); ScanSite has the same tendency when using high stringency; ScanSite only predicts Tyr-177 as a potential phosphorylation site.

For the reasons given above, mass spectrometry-based approaches usually provide data that allow conclusions about the presence but not the absence of phosphorylation sites. Thus it is not possible to conclude that a bioinformatic algorithm overpredicts as it might very well be that particular sites

are phosphorylated but are not observed for various reasons. Nevertheless it can be stated that several phosphorylation sites are also missed by NetPhos and ScanSite using medium or low stringency thresholds. For instance, NetPhos predicted only four of the nine tyrosine phosphorylation sites, whereas ScanSite predicted five of the nine experimentally determined phosphorylation sites. These results confirm the notion that the results of the currently used prediction programs have to be assessed with caution, and experimental validation is always required.

CONCLUSION AND PERSPECTIVE

Tyrosine-phosphorylated p185 Bcr/Abl was purified using immunoprecipitation with anti-phosphotyrosine antibody prior to SDS-PAGE. The tryptic digest of this purified protein was prefractionated on POROS R2/OLIGO R3 microcolumns and subjected to phosphotyrosine mapping by PSI scanning. In total nine different phosphorylated tyrosine residues were unambiguously localized in 12 different precursor ions: the POROS R2 fractions contained eight different tyrosine-phosphorylated peptides localizing six distinct phosphotyrosine residues; the OLIGO R3 fractions included four different phosphotyrosine-containing peptides allowing the assignment of five tyrosine phosphorylation sites (two of these phosphorylation sites confirmed the results obtained from the POROS R2 fraction). This indicates excellent sensitivity and applicability of PSI scanning for phosphotyrosine mapping when only limited sample amounts are available.

The nine characterized phosphorylated tyrosine residues correspond to three previously described phosphotyrosine residues in addition to six novel tyrosine phosphorylation sites, most of which were not predicted by currently used programs for the prediction of phosphotyrosine motifs even at permissive settings. This shows the need for unbiased experimental approaches for phosphorylation site mapping such as PSI scanning. The phosphopeptides analyzed in this study ranged in mass from less than 1 kDa to about 3.2 kDa with charge states between 2+ and 5+. Only the high accuracy and high resolution, provided by quadrupole time-of-flight-type tandem mass spectrometers, permitted the interpretation of the product ion spectrum of the quintuply and quadruply charged peptide and the unambiguous assignment of the fragment ion at this sensitivity level.

Another recently published study, which identified numerous tyrosine phosphorylation sites in Bcr, Abl, and/or Bcr/Abl, corroborated several tyrosine phosphorylation sites described in our study, thereby validating our approach of overexpressing the protein of interest, *i.e.* demonstrating that the sites found in our study are not mere artifacts of the overexpression of p185 in 293T cells. Ongoing functional studies are directed at discovering biological functions of the tyrosine phosphorylation sites found in these studies and in particular of those found in only one of the two studies, *i.e.* Tyr-515, Tyr-632, and Tyr-869. Furthermore additional experiments are

required using e.g. different proteolytic enzymes to obtain an even more comprehensive phosphotyrosine map of the protein in this state as one-quarter of all phosphotyrosine-containing peptides are too small or too large to be detected by the method applied using trypsin as the only protease.

Acknowledgments—We thank the group members and Bernhard Kuster (Cellzome, Heidelberg, Germany) for fruitful and stimulating discussions and Dr. Judith Jebanathirajah (Harvard Medical School, Boston, Massachusetts) for critically reading this manuscript.

* The work in the Mann laboratory was financed by a generous grant from the Danish National Research Foundation to the Center for Experimental Bioinformatics (CEBI). The costs of publication of this article were defrayed in part by the payment of page charges. This article must therefore be hereby marked "advertisement" in accordance with 18 U.S.C. Section 1734 solely to indicate this fact.

‡ Present address: Dept. of Cell Biology, Harvard Medical School, 240 Longwood Ave., Boston, MA 02115.

¶ Present address: Carl C. Icahn Center for Gene Therapy and Molecular Medicine and Dept. of Medicine, Division of Hematology, Oncology, Mount Sinai School of Medicine, New York, NY 10029.

|| To whom correspondence may be addressed: Inst. of Genetic Medicine, Johns Hopkins University School of Medicine, 2-127 Jefferson St. Bldg., 600 North Wolfe St., Baltimore, MD 21287. E-mail: pandey@jhmi.edu.

** To whom correspondence may be addressed: Center for Experimental Bioinformatics, Dept. of Biochemistry and Molecular Biology, University of Southern Denmark, Campusvej 55, 5230 Odense M, Denmark. E-mail: mann@bmb.sdu.dk.

REFERENCES

- Eckhart, W., Hutchinson, M. A., and Hunter, T. (1979) An activity phosphorylating tyrosine in polyoma T antigen immunoprecipitates. *Cell* **18**, 925–933
- Hunter, T., and Sefton, B. (1980) Transforming gene product of Rous sarcoma virus phosphorylates tyrosine. *Proc. Natl. Acad. Sci. U. S. A.* **77**, 1311–1315
- Hunter, T. (1998) The Croonian Lecture 1997. The phosphorylation of proteins on tyrosine: its role in cell growth and disease. *Philos. Trans. R. Soc. Lond. B Biol. Sci.* **353**, 583–605
- Blume-Jensen, P., and Hunter, T. (2001) Oncogenic kinase signalling. *Nature* **411**, 355–365
- Persson, C., Carballeira, N., Wolf-Watz, H., and Fallman, M. (1997) The PTPase YopH inhibits uptake of Yersinia, tyrosine phosphorylation of p130Cas and FAK, and the associated accumulation of these proteins in peripheral focal adhesions. *EMBO J.* **16**, 2307–2318
- Black, D. S., and Bliska, J. B. (1997) Identification of p130Cas as a substrate of Yersinia YopH (Yop51), a bacterial protein tyrosine phosphatase that translocates into mammalian cells and targets focal adhesions. *EMBO J.* **16**, 2730–2744
- Steen, H., Kuster, B., Fernandez, M., Pandey, A., and Mann, M. (2001) Detection of tyrosine phosphorylated peptides by precursor ion scanning quadrupole TOF mass spectrometry in positive ion mode. *Anal. Chem.* **73**, 1440–1448
- Steen, H., Kuster, B., and Mann, M. (2001) Quadrupole time-of-flight versus triple-quadrupole mass spectrometry for the determination of phosphopeptides by precursor ion scanning. *J. Mass Spectrom.* **36**, 782–790
- Steen, H., Kuster, B., Fernandez, M., Pandey, A., and Mann, M. (2002) Tyrosine phosphorylation mapping of the epidermal growth factor receptor signaling pathway. *J. Biol. Chem.* **277**, 1031–1039
- Hinsby, A. M., Olsen, J. V., Bennett, K. L., and Mann, M. (2003) Signaling initiated by overexpression of the fibroblast growth factor receptor-1 investigated by mass spectrometry. *Mol. Cell. Proteomics* **2**, 29–36
- Shtivelman, E., Lifshitz, B., Gale, R. P., and Canaani, E. (1985) Fused transcript of abl and bcr genes in chronic myelogenous leukaemia. *Nature* **315**, 550–554
- O'Dwyer, M. E., and Druker, B. J. (2000) Status of bcr-abl tyrosine kinase inhibitors in chronic myelogenous leukemia. *Curr. Opin. Oncol.* **12**, 594–597
- Ghaffari, S., Daley, G. Q., and Lodish, H. F. (1999) Growth factor independence and BCR/ABL transformation: promise and pitfalls of murine model systems and assays. *Leukemia* **13**, 1200–1206
- Vigneri, P., and Wang, J. Y. (2001) Induction of apoptosis in chronic myelogenous leukemia cells through nuclear entrapment of BCR-ABL tyrosine kinase. *Nat. Med.* **7**, 228–234
- Zimmermann, J., Buchdunger, E., Mett, H., Meyer, T., and Lydon, N. B. (1997) Potent and selective inhibitors of the Abl-kinase: phenylamino-pyrimidine (PAP) derivatives. *Bioorg. Med. Chem. Lett.* **7**, 187–192
- Schindler, T., Bornmann, W., Pellicena, P., Miller, W. T., Clarkson, B., and Kuriyan, J. (2000) Structural mechanism for STI-571 inhibition of abelson tyrosine kinase. *Science* **289**, 1938–1942
- Steen, H., Pandey, A., Andersen, J. S., and Mann, M. (2002) Analysis of tyrosine phosphorylation sites in signaling molecules by a phosphotyrosine-specific ammonium ion scanning method. *Science's STKE* http://stke.sciencemag.org/cgi/content/full/OC_sigtrans;2002/154/pl16
- Shevchenko, A., Wilm, M., Vorm, O., and Mann, M. (1996) Mass spectrometric sequencing of proteins from silver-stained polyacrylamide gels. *Anal. Chem.* **68**, 850–858
- Neubauer, G., and Mann, M. (1999) Mapping of phosphorylation sites of gel-isolated proteins by nanoelectrospray tandem mass spectrometry: potentials and limitations. *Anal. Chem.* **71**, 235–242
- Pendergast, A. M., Quilliam, L. A., Cripe, L. D., Bassing, C. H., Dai, Z., Li, N., Batzer, A., Rabun, K. M., Der, C. J., and Schlessinger, J. (1993) BCR-ABL-induced oncogenesis is mediated by direct interaction with the SH2 domain of the GRB-2 adaptor protein. *Cell* **75**, 175–185
- Liu, J., Wu, Y., Ma, G. Z., Lu, D., Haataja, L., Heisterkamp, N., Groffen, J., and Arlinghaus, R. B. (1996) Inhibition of Bcr serine kinase by tyrosine phosphorylation. *Mol. Cell. Biol.* **16**, 998–1005
- Sun, T. T., Campbell, M., Gordon, W., and Arlinghaus, R. B. (2001) Preparation and application of antibodies to phosphoamino acid sequences. *Biopolymers* **60**, 61–75
- Wilm, M., Neubauer, G., and Mann, M. (1996) Parent ion scans of unseparated peptide mixtures. *Anal. Chem.* **68**, 527–533
- Schmidt, G., Sehr, P., Wilm, M., Selzer, J., Mann, M., and Aktories, K. (1997) Gln 63 of Rho is deamidated by Escherichia coli cytotoxic necrotizing factor-1. *Nature* **387**, 725–729
- Schlosser, A., Pipkorn, R., Bossemeyer, D., and Lehmann, W. D. (2001) Analysis of protein phosphorylation by a combination of elastase digestion and neutral loss tandem mass spectrometry. *Anal. Chem.* **73**, 170–176
- Benore-Parsons, M., Seidah, N. G., and Wennogle, L. P. (1989) Substrate phosphorylation can inhibit proteolysis by trypsin-like enzymes. *Arch. Biochem. Biophys.* **272**, 274–280
- Brasher, B. B., and Van Etten, R. A. (2000) c-Abl has high intrinsic tyrosine kinase activity that is stimulated by mutation of the Src homology 3 domain and by autophosphorylation at two distinct regulatory tyrosines. *J. Biol. Chem.* **275**, 35631–35637
- Mann, M., and Jensen, O. N. (2003) Proteomic analysis of post-translational modifications. *Nat. Biotechnol.* **21**, 255–261
- Salomon, A. R., Ficarro, S. B., Brill, L. M., Brinker, A., Phung, Q. T., Ericson, C., Sauer, K., Brock, A., Horn, D. M., Schultz, P. G., and Peters, E. C. (2003) Profiling of tyrosine phosphorylation pathways in human cells using mass spectrometry. *Proc. Natl. Acad. Sci. U. S. A.* **100**, 443–448
- Blom, N., Gammeltoft, S., and Brunak, S. (1999) Sequence and structure-based prediction of eukaryotic protein phosphorylation sites. *J. Mol. Biol.* **294**, 1351–1362
- Yaffe, M. B., Leparac, G. G., Lai, J., Obata, T., Volinia, S., and Cantley, L. C. (2001) A motif-based profile scanning approach for genome-wide prediction of signaling pathways. *Nat. Biotechnol.* **19**, 348–353